JCI insight

Piezo1 incorporates mechanical force signals into the genetic program that governs lymphatic valve development and maintenance

Dongwon Choi, … , Il-Taeg Cho, Young-Kwon Hong

JCI Insight. 2019;4(5):e125068. https://doi.org/10.1172/jci.insight.125068.

Research Article **Vascular biology**

The lymphatic system plays crucial roles in tissue homeostasis, lipid absorption, and immune cell trafficking. Although lymphatic valves ensure unidirectional lymph flows, the flow itself controls lymphatic valve formation. Here, we demonstrate that a mechanically activated ion channel Piezo1 senses oscillating shear stress (OSS) and incorporates the signal into the genetic program controlling lymphatic valve development and maintenance. Time-controlled deletion of *Piezo1* using a pan-endothelial Cre driver (*Cdh5[PAC]-CreER^{T2}*) or lymphatic-specific Cre driver (*Prox1-CreER^{T2}*) equally inhibited lymphatic valve formation in newborn mice. Furthermore, *Piezo1* deletion in adult lymphatics caused substantial lymphatic valve degeneration. *Piezo1* knockdown in cultured lymphatic endothelial cells (LECs) largely abrogated the OSS-induced upregulation of the lymphatic valve signature genes. Conversely, ectopic Piezo1 overexpression upregulated the lymphatic valve genes in the absence of OSS. Remarkably, activation of Piezo1 using chemical agonist Yoda1 not only accelerated lymphatic valve formation in animals, but also triggered upregulation of some lymphatic valve genes in cultured LECs without exposure to OSS. In summary, our studies together demonstrate that Piezo1 is the force sensor in the mechanotransduction pathway controlling lymphatic valve development and maintenance, and Piezo1 activation is a potentially novel therapeutic strategy for congenital and surgery-associated lymphedema.

JCI insight

RESEARCH ARTICLE

Piezo1 incorporates mechanical force signals into the genetic program that governs lymphatic valve development and maintenance

Dongwon Choi,[1,2] Eunkyung Park,[1,2] Eunson Jung,[1,2] Boksik Cha,[3] Somin Lee,[4] James Yu,[4] Paul M. Kim,[1,2] Sunju Lee,[1,2] Yeo Jin Hong,[1,2] Chester J. Koh,[5] Chang-Won Cho,[1,6] Yifan Wu,[1,2] Noo Li Jeon,[4] Alex K. Wong,[1] Laura Shin,[1] S. Ram Kumar,[1] Ivan Bermejo-Moreno,[7] R. Sathish Srinivasan,[3] Il-Taeg Cho,[1] and Young-Kwon Hong[1,2]

[1]Department of Surgery, and [2]Department of Biochemistry and Molecular Medicine, Norris Comprehensive Cancer Center, Keck School of Medicine, University of Southern California, Los Angeles, California, USA. [3]Cardiovascular Biology Research Program, Oklahoma Medical Research Foundation, Oklahoma City, Oklahoma, USA. [4]Department of Mechanical and Aerospace Engineering, Seoul National University, Seoul, South Korea. [5]Division of Pediatric Urology, Texas Children's Hospital, Baylor Collexge of Medicine, Houston, Texas, USA. [6]Traditional Food Research Group, Korea Food Research Institute, Wanju-gun, Jeollabuk-do, South Korea. [7]Department of Aerospace and Mechanical Engineering, University of Southern California, Los Angeles, California, USA.

The lymphatic system plays crucial roles in tissue homeostasis, lipid absorption, and immune cell trafficking. Although lymphatic valves ensure unidirectional lymph flows, the flow itself controls lymphatic valve formation. Here, we demonstrate that a mechanically activated ion channel Piezo1 senses oscillating shear stress (OSS) and incorporates the signal into the genetic program controlling lymphatic valve development and maintenance. Time-controlled deletion of *Piezo1* using a pan-endothelial Cre driver (*Cdh5[PAC]-CreER^{T2}*) or lymphatic-specific Cre driver (*Prox1-CreER^{T2}*) equally inhibited lymphatic valve formation in newborn mice. Furthermore, *Piezo1* deletion in adult lymphatics caused substantial lymphatic valve degeneration. *Piezo1* knockdown in cultured lymphatic endothelial cells (LECs) largely abrogated the OSS-induced upregulation of the lymphatic valve signature genes. Conversely, ectopic Piezo1 overexpression upregulated the lymphatic valve genes in the absence of OSS. Remarkably, activation of Piezo1 using chemical agonist Yoda1 not only accelerated lymphatic valve formation in animals, but also triggered upregulation of some lymphatic valve genes in cultured LECs without exposure to OSS. In summary, our studies together demonstrate that Piezo1 is the force sensor in the mechanotransduction pathway controlling lymphatic valve development and maintenance, and Piezo1 activation is a potentially novel therapeutic strategy for congenital and surgery-associated lymphedema.

Introduction

The lymphatic system controls tissue fluid homeostasis, immune cell trafficking, and lipid absorption. Lymphatic valves ensure a unidirectional flow of lymph fluid in lymphatic vessels. Dysfunctional or malformed lymphatic valves significantly impair fluid drainage, immune responses, and lipid uptake in the gut (1–4). Fluid flow–generated mechanical force regulates mechanotransduction pathways that incorporate the flow-induced shear stress signals into genetic programs that govern development and function of the vascular system (5–8). Previous studies have dissected mechanotransduction pathways that control different aspects of vascular pathophysiology (9–14). In particular, recent work has elegantly identified and characterized important molecular constituents in lymphatic valve formation (15–22). Notably, these molecular players, intricately controlled by fluid flow–generated oscillating shear stress (OSS), cooperatively orchestrate the genetic and epigenetic programs responsible for the development, function, and maintenance of lymphatic valves.

Piezo proteins, encoded by Piezo1 and Piezo2, were originally identified as pore-forming subunits of mechanically activated ion channels (23, 24). Piezo1 has subsequently been demonstrated to be a cell stretch

Conflict of interest: The authors have declared that no conflict of interest exists.

Submitted: September 21, 2018
Accepted: January 17, 2019
Published: March 7, 2019

Reference information:
JCI Insight. 2019;4(5):e125068.
https://doi.org/10.1172/jci.insight.125068.

sensor that integrates physiological force into vascular architecture, functioning as a critical molecular player for vascular development and function (23–27). Patient-based studies have recently associated mutations in the *PIEZO1* gene with generalized lymphatic dysplasia and dysfunction (28–30). Despite the strong clinical associations, the role of Piezo1 in a mechanotransduction that controls lymphatic development, maintenance, and function is largely unknown. In this paper, we aimed to elucidate the function of Piezo1 in embryonic and postnatal lymphatic growth and valve development. Based on the data presented here, we propose that Piezo1 functions as a force sensor of the mechanotransduction that delivers hemodynamic signals from oscillating fluid flow to a genetic program that regulates lymphatic valve formation and maintenance.

Results

Piezo1 is essential for lymphatic valve development. We set out to investigate the effect of *Piezo1* knockout (KO) on lymphatic valve formation by inducing conditional deletion of *Piezo1* in lymphatic endothelial cells (LECs). For this goal, we produced mouse pups harboring a combination of *Prox1-CreER^{T2}* (19), *Prox1-tdTomato* (31), and/or *Piezo1$^{fl/fl}$* (32) alleles. Lymphatic *Piezo1* deletion (Piezo1$^{\Delta LEC}$) was then induced in these pups at postnatal day 1 (P1) by tamoxifen injection, and subsequently, lymphatic valve formation in the mesentery and tail skin was analyzed at P7 (Figure 1A). Mesenteric lymphatic valves, clearly marked with strong tdTomato expression because of high expression of Prox1 in lymphatic valve leaflet LECs, were normally formed at vascular branch points of the control animals. In the lymphatic *Piezo1*-KO pups, however, not only were mesenteric lymphatic vessels scarce in terms of their density, but they also lacked mature valves at the branching points (Figure 1, B–I). Accordingly, the total numbers of valves (matured and immatured) were significantly reduced by *Piezo1* deletion in both jejunum and colon (Figure 1, R and S). Moreover, high-powered images identified that, while all the control valves appeared to be fully mature, Piezo1-deleted mice demonstrated immature valves that were arrested at different stages of valve development (ref. 16 and Figure 1, J–M). We could detect the absence of lymphatic valve–forming activity at the expected valve branching points (Figure 1, E and I), constriction of vessels (Figure 1L), and immature valve leaflets (Figure 1M). This observation raised a possibility that Piezo1 may be essential for many stages of lymphatic valve development. Furthermore, we could also detect defective lymphatic valve formation in the tail skin after *Piezo1* deletion (Figure 1, N–S). Notably, these conditional lymphatic *Piezo1*-KO pups exhibited a substantially retarded body growth (Supplemental Figure 1; supplemental material available online with this article; https://doi.org/10.1172/jci.insight.125068DS1). To confirm these phenotypes using an independent Cre allele, we next used the *Cdh5(PAC)-CreER^{T2}* line (33). Because Cdh5/vascular endothelial cadherin is expressed in nearly all ECs (34), this Cre allele was expected to induce *Piezo1* deletion in both blood and LECs. Using this driver line, *Piezo1* was deleted at P3, and its consequence on lymphatic valve formation was studied at P10 (Figure 1T). Indeed, *Piezo1* ablation by the *Cdh5(PAC)-CreER^{T2}* allele inhibited lymphatic valve formation (Figure 1, U and V, and Supplemental Figure 2).

As mentioned above, *Piezo1* deletion also reduced lymphatic vessel density, possibly by suppressing lymphatic vessel growth or sprouting (Figure 1, B–I, and Supplemental Figure 3). We thus hypothesized that Piezo1 may be expressed not only in lymphatic valves (valvular LECs), but also in lymphatic vessels (luminal LECs). To date, the expression pattern of Piezo1 in the lymphatics in vivo has not been clearly documented. We therefore investigated the expression pattern of Piezo1 in valvular and luminal LECs using a Piezo1 reporter mouse, Piezo1^{P1-tdT}, which encodes a C-terminus fusion protein of Piezo1 with tdTomato protein (26). This reporter mouse, combined with immunofluorescence assays, showed that both valvular and luminal LECs express Piezo1 with much stronger expression in the valvular leaflet LECs (Figure 2, A–D).

We next asked whether lymphatic valve formation might have been prevented by defective lymphangiogenesis in *Piezo1*-KO animals. Although a lymphatic valve–specific Cre line would be the most desirable tool to delete *Piezo1* exclusively in valvular LECs, but not in luminal LECs, no animal model has been established offering such selectivity. Therefore, we set out to deal with this technical limitation by significantly reducing tamoxifen dosage: Because Prox1 expression is 5–10 times higher in valvular LECs than luminal LECs (35, 36), CreER^{T2} protein encoded by the *Prox1-CreER^{T2}* allele is much more abundant in valvular LECs than luminal LECs. We thus speculate that, at low-dose tamoxifen, *Piezo1* deletion by *Prox1-CreER^{T2}* allele would occur more readily in valvular LECs than luminal LECs. Indeed, a one-fifth dose of the routine tamoxifen concentration (15 mg/kg) suppressed lymphatic valve formation in the *Piezo1*-KO pups without significantly affecting lymphatic vessel density (Figure 2, E–N, and Supplemental Figure 4). Together, these data indicate that Piezo1 is essential for lymphatic valve formation, possibly functioning at different stages of lymphatic valve development.

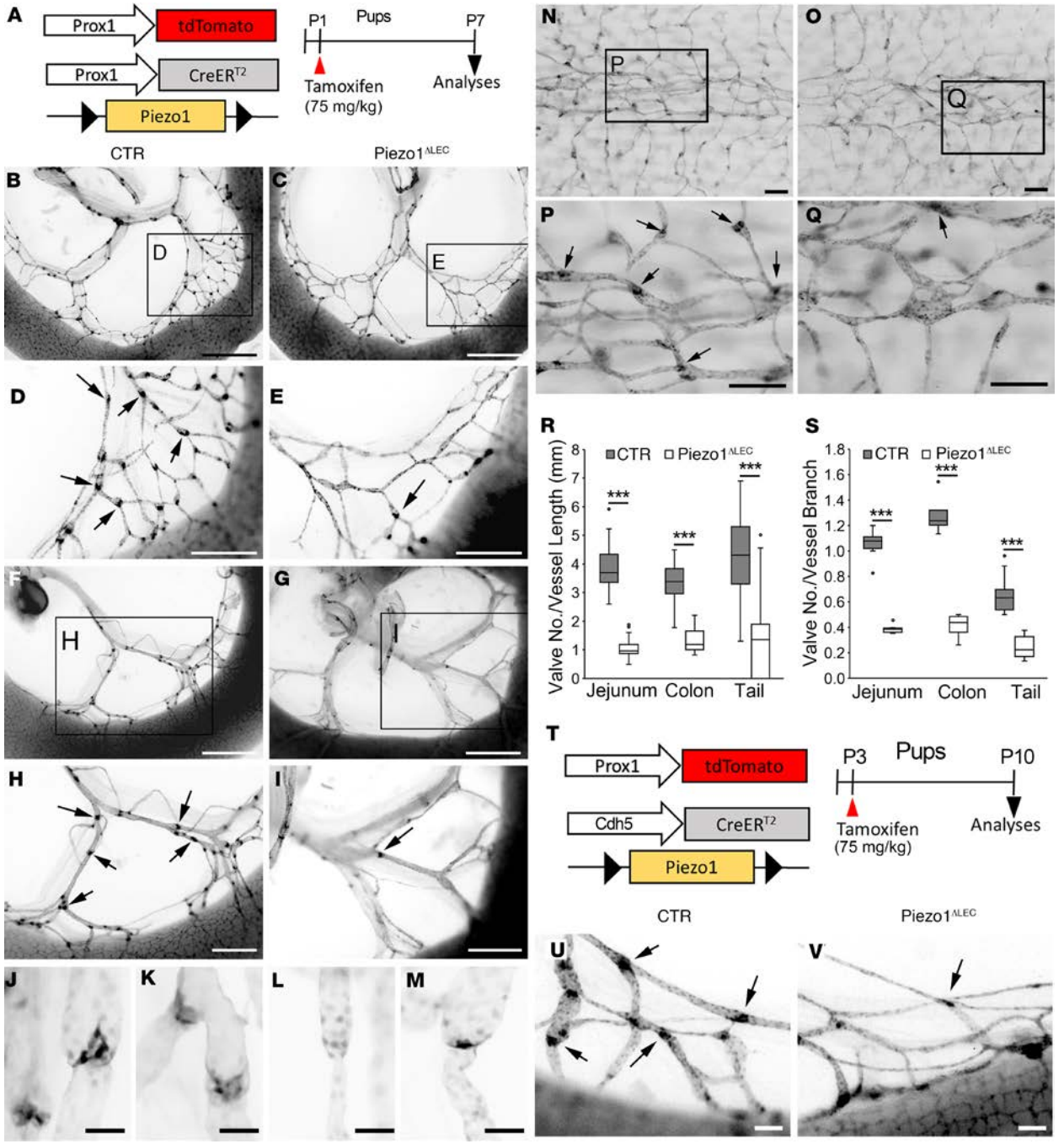

Figure 1. Piezo1 is essential for lymphatic valve development. (**A**–**S**) Effect of lymphatic deletion of *Piezo1* on lymphatic valve development. (**A**) Experimental design. Control pups (CTR) harbor *Prox1-tdTomato* and *Prox1-CreER*^{T2}, but lack the *Piezo1*$^{fl/fl}$ allele, while lymphatic *Piezo1*-KO pups (Piezo1$^{\Delta LEC}$) have all *Prox1-tdTomato*, *Prox1-CreER*^{T2}, and *Piezo1*$^{fl/fl}$. Tamoxifen (75 mg/kg) was s.c. injected into pups at P1, and tissues were harvested and analyzed at P7. (**B**–**I**) Mesenteric lymphatics in the (**B**–**E**) jejunum or (**F**–**I**) colon are shown in the (**B**, **D**, **F**, and **H**) CTR or (**C**, **E**, **G**, and **I**) lymphatic *Piezo1*-KO pups. High-magnification images of mesenteric lymphatic valves of (**J** and **K**) CTR and (**L** and **M**) *Piezo1*-KO pups are also shown. (**N**–**Q**) Dermal lymphatic valve development was impaired in the tail skin of the lymphatic *Piezo1*-KO pups. (**R** and **S**) Box-and-whisker plots showing lymphatic valve number (**R**) per lymphatic vessel length or (**S**) per branching point in the jejunum, colon, and tail. The box plots depict the minimum and maximum values (whiskers), the upper and lower quartiles, and the median. The length of the box represents the interquartile range. (**T**–**V**) Impact of endothelial deletion of *Piezo1* using a *Cdh5(PAC)-CreER*^{T2} driver of lymphatic valve development. (**T**) Experimental design: *Peizo1* deletion was induced in pups [*Prox1-tdTomato*, *Cdh5(PAC)-CreER*^{T2}, and/or *Piezo1*$^{fl/fl}$] at P3 by i.p. tamoxifen injection (75 mg/kg), and the mesenteric lymphatic valves in the jejunum were analyzed at P10. (**U** and **V**) Endothelial *Piezo1* deletion significantly inhibited lymphatic valve formation. All images of lymphatic vessels and valves were captured based on the *tdTomato* signal and shown in inverted grayscales. Boxed areas were enlarged in panels below, respectively. Arrows mark matured Prox1^{hi} lymphatic valves. Scale bars: 1 mm (**B**, **C**, **F**, and **G**); 500 μm (**D**, **E**, **H**, and **I**); 50 μm (**J**–**M**); 200 μm (**N**–**Q**); and 100 μm (**U** and **V**). ***$P < 0.001$, unpaired, 2-tailed *t* test compared with the valve of the controls. More than 5 pups were used for each group. A representative of >10 images was chosen for each panel.

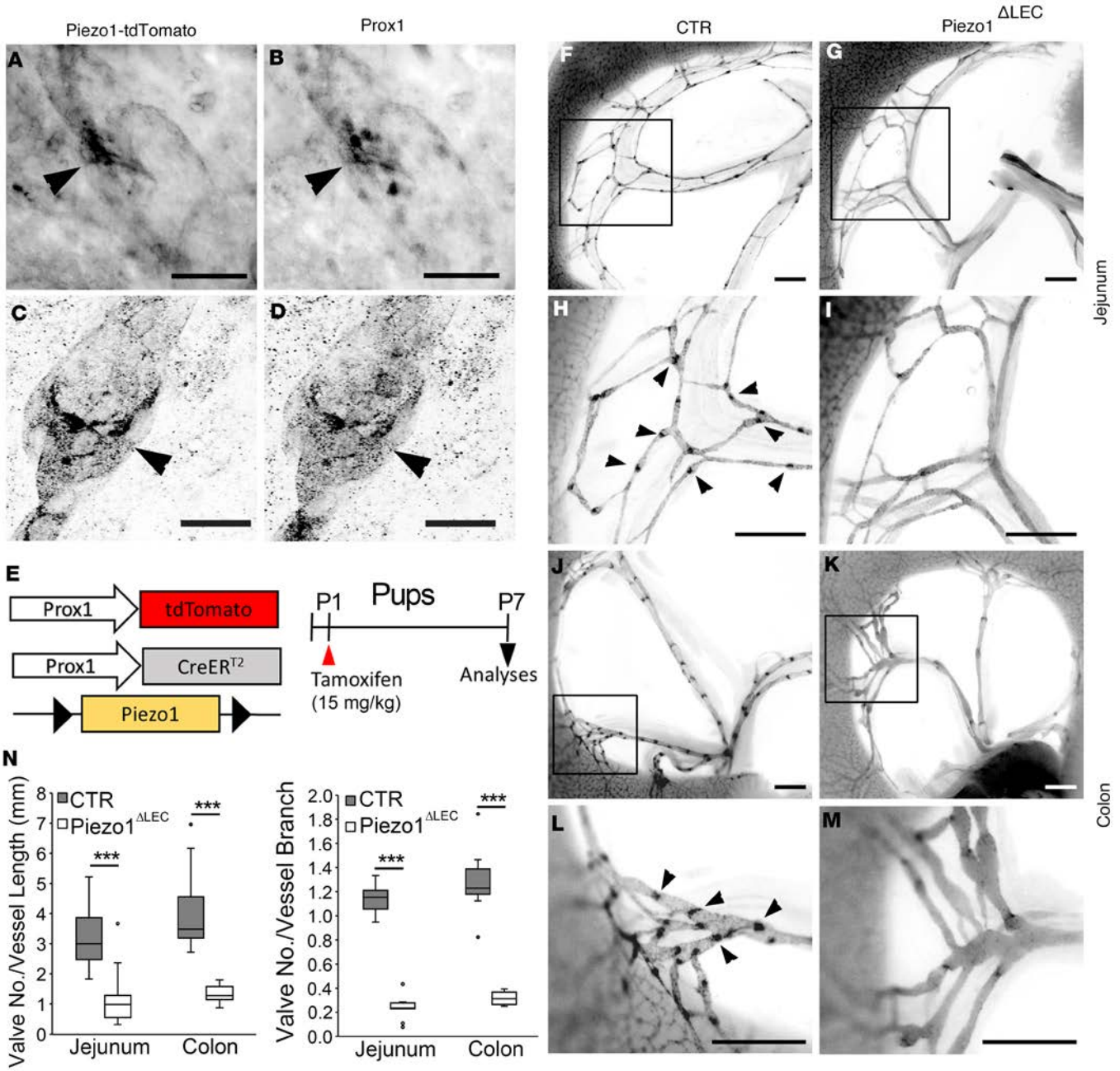

Figure 2. *Piezo1* deletion in lymphatic valves by low-dose tamoxifen. (**A**–**D**) Dermal lymphatics in the ear of *Piezo1-tdTomato* adult reporter mouse *Piezo1*$^{P1\text{-}tdT}$ (26) were immunostained for tdTomato protein (to amplify the reporter signal) and Prox1 (to detect LECs). Images were captured by an (**A** and **B**) epifluorescence or (**C** and **D**) confocal microscope. Note an enriched expression of Piezo1-tdTomato fusion protein in Prox1^{hi} valve leaflet LECs. (**E**–**N**) *Piezo1* deletion by low-dose tamoxifen suppressed lymphatic valve formation with a minimal effect on lymphatic vessel density. (**E**) Experimental design: *Peizo1* deletion was induced by low-dose tamoxifen injection (15 mg/kg) in the control and lymphatic *Piezo1*-KO pups at P1, and the mesenteric lymphatic valves in the jejunum and colon were analyzed at P7. (**F**–**M**) *Piezo1* deletion suppressed lymphatic valve formation in the mesenteries of the (**F**–**I**) jejunum and (**J**–**M**) colon. Boxed areas were enlarged in panels below, respectively. Arrows mark matured lymphatic valves. (**N**) Quantitation of lymphatic valves in the control and lymphatic *Piezo1*-KO pups for panels **F**–**M**. The box plots depict the minimum and maximum values (whiskers), the upper and lower quartiles, and the median. The length of the box represents the interquartile range. The lymphatics were visualized by Prox1-tdTomato, and the signal was expressed in inverted grayscale. Scale bars: 100 μm (**A**–**D**), 500 μm (**F**–**M**). ***$P < 0.001$, unpaired, 2-tailed *t* test compared with the valve of the controls. Three pups were used for each group. A representative of >10 images was chosen for each panel.

Piezo1 deletion leads to degeneration of lymphatic valves in adults. We next asked whether Piezo1 function is continuously needed to maintain lymphatic valves after development. Lymphatic *Piezo1* deletion was induced at day 21 (juvenile), and the integrity of lymphatic valves in the skin and mesentery was investigated at day 49 (adult) (Figure 3A). We first examined matured lymphatic collectors that run along with the saphenous vein in the hind limb of the control and *Piezo1*-mutant mice. Notably, postdevelopmental lymphatic *Piezo1* deletion caused significant degeneration of both lymphatic valves and lymphatic vessels in the skin (Figure 3, B–G, L, M). These lymphatic atrophies were also detected in the mesentery, where the lymphatics of *Piezo1*-deficient mice were much thinner and scarce, with fewer valves, compared with those of the control mice (Figure 3, H–M). Together, these data suggest that Piezo1 function is continuously necessary to maintain the integrity of lymphatic vessels and valves in adults.

Piezo1 is required for the OSS-mediated upregulation of lymphatic valve genes. The in vivo lymphatic phenotypes of *Piezo1*-KO animals led us to investigate the mechanotransduction mechanism for the lymphatic valve formation. Fluid flow is known to play a key role in vascular development and morphogenesis (5). In particular, OSS has been reported to upregulate the lymphatic valve–associated genes, such as FOXC2, GATA2, CX37, LAMA5, and ITGA9, and to induce cellular morphology change (15–22). We thus investigated how the mechanosensor Piezo1 affects the mechanotransduction process by performing in vitro loss-of-function studies. Consistent with the previous reports (15–20), OSS changed the morphology of cultured primary human LECs to more cuboidal shapes (Figure 4, A and B, and Supplemental Figure 5) and upregulated the lymphatic valve–associated genes mentioned above (Figure 4, C and D, and Supplemental Figure 6). Remarkably, the OSS-induced upregulation of these genes was largely abrogated by Piezo1 knockdown (Figure 4, E and F, and Supplemental Figure 7). Notably, upregulation of ITGA9 by OSS was not affected by Piezo1 knockdown. Together, these loss-of-function studies suggest that Piezo1 plays a key role in the OSS-activated mechanotransduction that regulates lymphatic valve gene expression.

Ectopic expression of Piezo1 triggers lymphatic valve gene expression profile. Conversely, we next asked whether Piezo1 gain of function could recapitulate the molecular phenotypes caused by OSS. We transfected primary LECs with a plasmid bicistronically encoding mouse Piezo1 and EGFP and then evaluated the expression of the lymphatic valve–associated genes. $EGFP^+$, thus overexpressing Piezo1, upregulated FOXC2, GATA2, CX37, and LAMA5 expression by 3- to 4-fold, in the absence of OSS (arrowheads, Figure 5, A and B). However, neighboring $EGFP^-$ (untransfected) LECs did not upregulate these genes (arrows, Figure 5, A and B). Notably, ITGA9 was not upregulated by Piezo1 expression. To confirm these data, LECs were transfected with a control or Piezo1-expressing vector and further cultured in the absence of OSS. Indeed, quantitative PCR (qPCR) and Western blot analyses revealed that overexpression of Piezo1 upregulated the expression of mRNA and protein of FOXC2, GATA2, CX37, and LAMA5 (Figure 5, C and D). ITGA9 expression was consistently unaltered. Together, these gain-of-function studies demonstrate that ectopic expression of Piezo1 was able to partly recapitulate the lymphatic valve gene profile in the absence of OSS.

Activation of Piezo1 accelerates lymphatic valve formation in a mouse model. The outcome of the in vitro gain-of-function study led us to investigate whether activation of Piezo1 promotes lymphatic valve formation in animals. Yoda1, identified as the first small chemical agonist of Piezo1, delays the inactivation phase of transient currents and sensitizes Piezo1 response to external mechanical stimuli (37). Thus, we asked whether Yoda1 treatment enhances lymphatic valve formation in vivo. Toward this goal, Yoda1, or vehicle alone, was injected into Prox1-EGFP mice at E18.5 (into pregnant females) and again at P0 (into newborns). The next day at P1, lymphatic valve formation was analyzed in the mesenteries of the jejunum and colon and in the tail skin of the control or Yoda1-treated pups (Figure 6A). While valve formation activity was not yet detected at the proximal regions of the mesentery lymphatics of the vehicle-treated jejunum, a number of lymphatic valves were already visible in the Yoda1-treated jejunum mesentery (Figure 6B). Similarly, Yoda1 accelerated lymphatic valve formation in the colon and tail skin: A higher number of lymphatic valves could be found in the Yoda1-treated pups (Figure 6, C and D). Yoda1 treatment significantly enhanced lymphatic valve formation in all the tissues tested (Figure 6, E and F). Together, we concluded that chemical activation of Piezo1 was sufficient to augment lymphatic valve development, possibly through sensitization of Piezo1 to lymphatic fluid flow in vivo.

Activation of Piezo1 in vitro upregulates some lymphatic valve genes without flow. We next asked whether Piezo1 activation using Yoda1 could upregulate any or all of the lymphatic valve signature genes in cultured LECs in the absence of fluid flow. Toward this aim, we treated cultured primary human LECs with

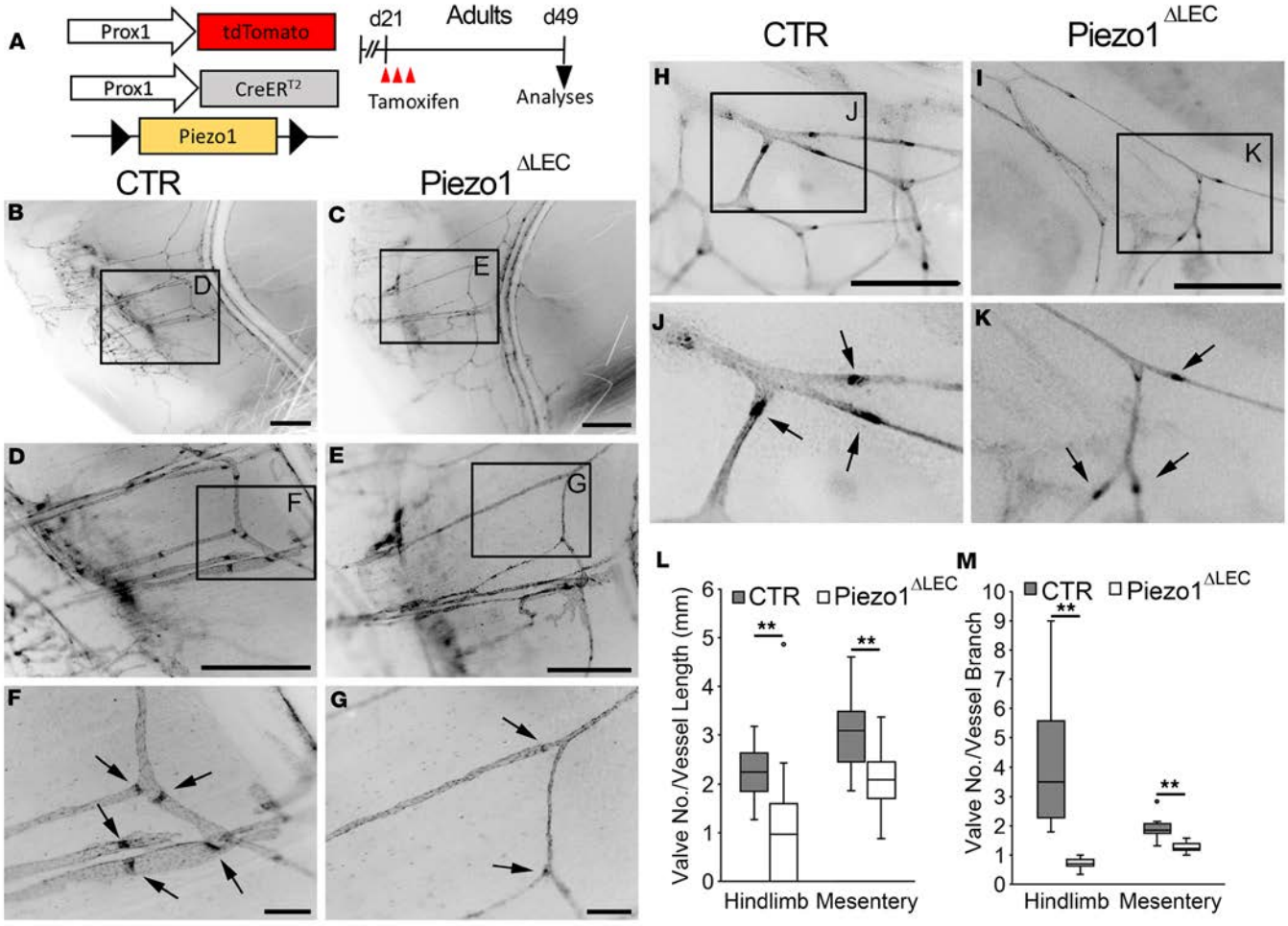

Figure 3. Piezo1 is required for lymphatic valve maintenance. (**A**) Experimental design. Tamoxifen (75 mg/kg) was i.p. injected into young adult mice every other day for a total of 3 times starting from day 21, and lymphatic valve maintenance was analyzed at day 49. Control mice, *Prox1-tdTomato* and *Prox1-CreER*^{T2}; lymphatic *Piezo1*-KO mice (Piezo1$^{\Delta LEC}$), *Prox1-tdTomato*, *Prox1-CreER*^{T2}, and *Piezo1*$^{fl/fl}$. (**B**–**G**) Overview and progressively enlarged images of collecting lymphatic vessels running next to the saphenous vein in the hind limb show (**B**, **D**, and **F**) healthy, mature valves in the control mice but (**C**, **E**, and **G**) degenerated valve remnants in lymphatic *Piezo1*-KO mice. (**H**–**K**) Mesenteric lymphatic vessels and valves in the (**H** and **J**) control mice and (**I** and **K**) lymphatic *Piezo1*-KO mice. (**L** and **M**) Box-and-whisker plots showing (**L**) lymphatic valve number per vessel length and (**M**) valve number per vessel branch. The box plots depict the minimum and maximum values (whiskers), the upper and lower quartiles, and the median. The length of the box represents the interquartile range. Scale bars: 1 mm (**B**–**E**, **H**, and **I**), 200 μm (**F** and **G**). $^{**}P < 0.01$, unpaired, 2-tailed *t* test. A representative of > 10 images was chosen for each panel. More than 5 adult mice were used for each group. No sex variations were found. Arrows mark lymphatic valves.

different doses of Yoda1 under the standard static condition. Indeed, Yoda1 treatment of LECs led to upregulation of both mRNA and protein of GATA2, CX37, LAMA5, and ITGA9 (Figure 7, A and B). Interesting, FOXC2 was rather slightly downregulated by increasing doses of Yoda1. Prox1 expression was not altered. Despite the reported EC_{50} of Yoda1 activation of Piezo1 in transfected HEK293 cells being about 20–25 μM (37), primary human LECs treated with Yoda1 higher than 1 μM for 24 hours revealed several signs of significant cytotoxicity, including cell detachment, cell-cell junction disruption, and cell contraction and spindle formation (data not shown). Moreover, we investigated whether the Yoda1-mediated upregulation of these lymphatic valve genes was mediated through Piezo1. LECs were transfected with siRNA for control or Piezo1 to knock down Piezo1 expression, and their expressions were determined using qPCR and Western blot analyses. Indeed, Piezo1 knockdown prevented Yoda1-induced upregulation of GATA2, CX37, and LAMA5 (Figure 7, C and D). Interestingly, however, Piezo1 knockdown did not affect Yoda1-induced ITGA9 expression. Together, these data suggest that chemical activation of Piezo1 using Yoda1 upregulates some of the lymphatic valve genes in the absence of mechanical force.

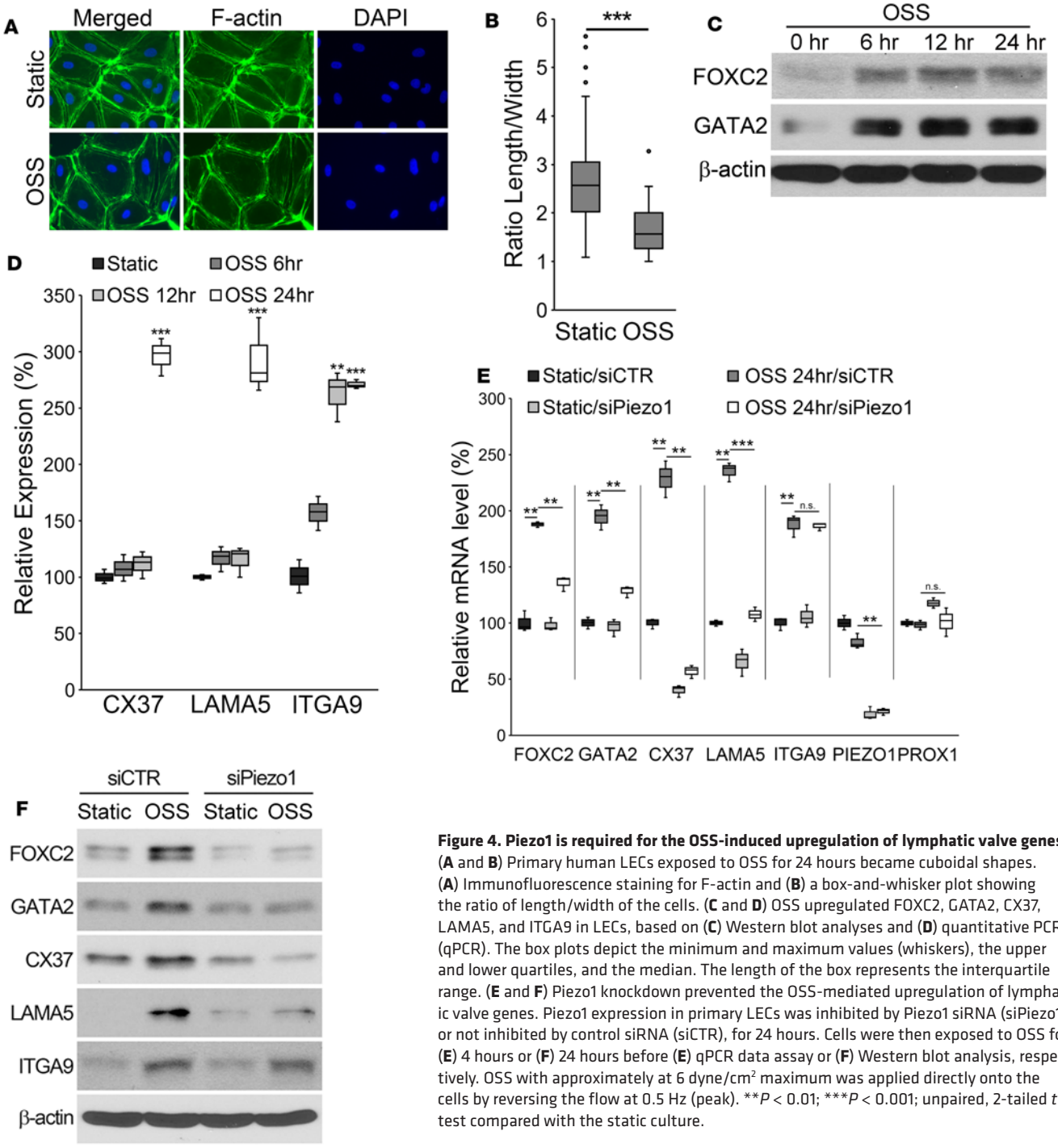

Figure 4. Piezo1 is required for the OSS-induced upregulation of lymphatic valve genes. (**A** and **B**) Primary human LECs exposed to OSS for 24 hours became cuboidal shapes. (**A**) Immunofluorescence staining for F-actin and (**B**) a box-and-whisker plot showing the ratio of length/width of the cells. (**C** and **D**) OSS upregulated FOXC2, GATA2, CX37, LAMA5, and ITGA9 in LECs, based on (**C**) Western blot analyses and (**D**) quantitative PCR (qPCR). The box plots depict the minimum and maximum values (whiskers), the upper and lower quartiles, and the median. The length of the box represents the interquartile range. (**E** and **F**) Piezo1 knockdown prevented the OSS-mediated upregulation of lymphatic valve genes. Piezo1 expression in primary LECs was inhibited by Piezo1 siRNA (siPiezo1), or not inhibited by control siRNA (siCTR), for 24 hours. Cells were then exposed to OSS for (**E**) 4 hours or (**F**) 24 hours before (**E**) qPCR data assay or (**F**) Western blot analysis, respectively. OSS with approximately at 6 dyne/cm^2 maximum was applied directly onto the cells by reversing the flow at 0.5 Hz (peak). $^{**}P < 0.01$; $^{***}P < 0.001$; unpaired, 2-tailed *t* test compared with the static culture.

Discussion

Lymphatic valves are essential for the unidirectional flow of interstitial fluid. Because of malformations or injuries, diseased lymphatic valves often lead to severe lymphatic pathologies. Recent studies demonstrated that fluid flow–derived physical signal significantly controls lymphatic valve development through mechanotransduction pathways and identified key molecular players essential for the pathways (15–22). In this study, we defined the crucial role of the cell stretch sensor Piezo1 in incorporating the flow-mediated physical signal into the genetic program controlling lymphatic valve development. Previous studies suggested that vascular ECs in vivo would be subjected to both fluid shear stress and cyclic cell stretch, and, when combined in vitro, these 2 physical stimuli appeared to synergistically deliver various vascular phenotypes,

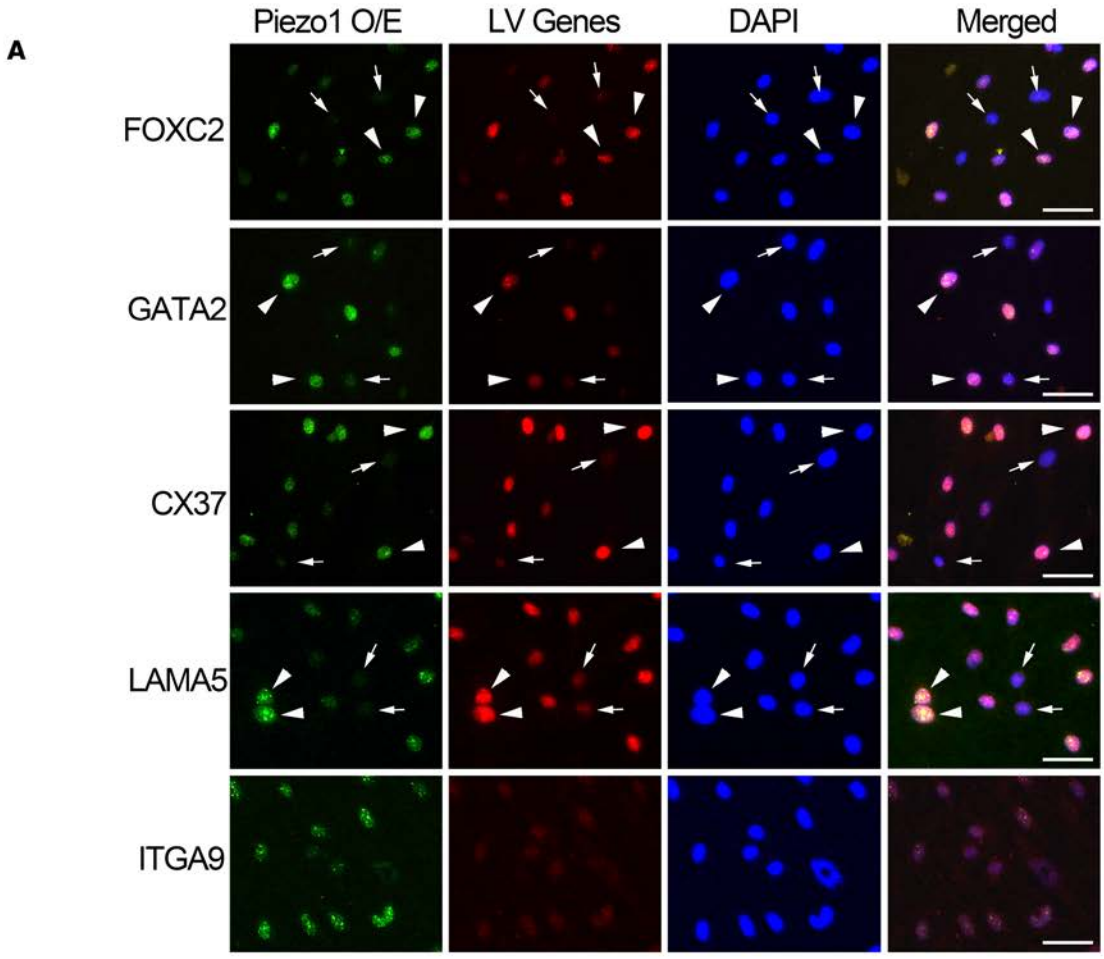
A
Piezo1 O/E
LV Genes
DAPI
Merged
FOXC2
GATA2
CX37
LAMA5
ITGA9

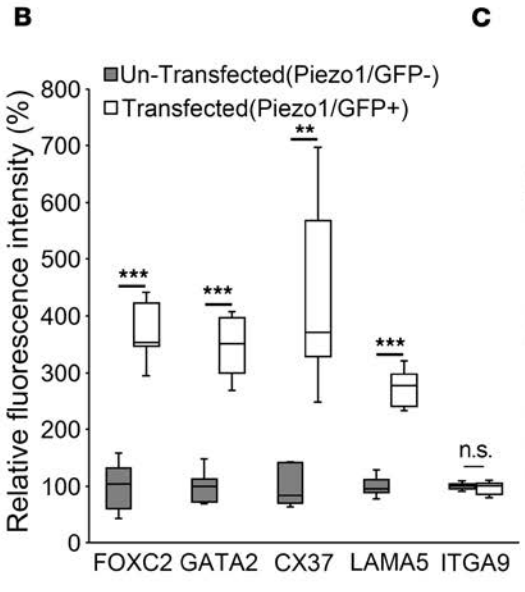
B
Un-Transfected(Piezo1/GFP-)
Transfected(Piezo1/GFP+)
Relative fluorescence intensity (%)
800
700
600
500
400
300
200
100
0
**
***
***
***
n.s.
FOXC2 GATA2 CX37 LAMA5 ITGA9

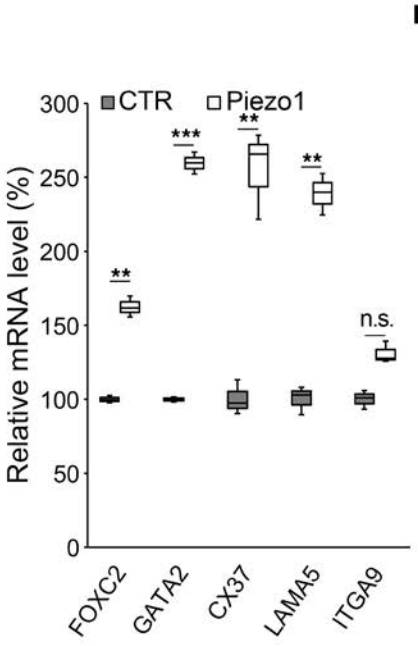
C
CTR
Piezo1
Relative mRNA level (%)
300
250
200
150
100
50
0
**
***
**
**
n.s.
FOXC2
GATA2
CX37
LAMA5
ITGA9

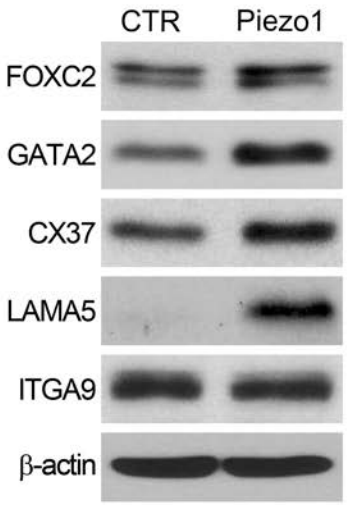
D
CTR
Piezo1
FOXC2
GATA2
CX37
LAMA5
ITGA9
β-actin

Figure 5. Ectopic expression of Piezo1 induces lymphatic valve signature genes. (**A** and **B**) Primary LECs were transfected with a Piezo1/EGFP-expressing plasmid and cultured for 48 hours without OSS, before immunostaining for lymphatic valve genes FOXC2, GATA2, CX37, LAMA5, and ITGA9. (**A**) Arrowheads point to transfected $EGFP^+$ (thus Piezo1-overexpressing) cells, whereas arrows point to $EGFP^-$, untransfected cells. O/E, overexpression; LV, lymphatic valve. (**B**) The intensity of these cells was measured and charted in a box-and-whisker plot. (**C** and **D**) Expression of the lymphatic valve genes in LECs that were transfected with a control (CTR) or Piezo1/EGFP-expressing plasmid (Piezo1) was determined by qRT-PCR after (**C**) 24 hours, or by Western blot assay after (**D**) 48 hours, in the absence of OSS. The box plots depict the minimum and maximum values (whiskers), the upper and lower quartiles, and the median. The length of the box represents the interquartile range. Scale bars: 50 μm (**A**). $^{**}P < 0.01$; $^{***}P < 0.001$; unpaired, 2-tailed *t* test compared with (**B**) the untransfected cells or (**C**) the control plasmid.

such as actin filament alignment and cell differentiation (38–41). Accordingly, we hypothesize that the OSS and cyclic cell stretching may be similarly sensed by Piezo1 and trigger the genetic program responsible for lymphatic valve formation. OSS may induce plasma membrane spreading and cytoskeletal rearrangement, similar to those effects created by cyclic cell stretching.

In this study, loss of function of Piezo1 in mice and in purified cells clearly demonstrated the essential role of Piezo1 in various stages of lymphatic valve development. To conditionally delete *Piezo1*, we used 2 Cre drivers that target nearly all ECs as well as selectively for lymphatic-lineage ECs (Figure 1). We also successfully targeted lymphatic valve ECs by lowering tamoxifen concentrations (Figure 2). Moreover, we induced *Piezo1* deletion in young adult mice to study the role of Piezo1 in matured lymphatic valves and found that matured lymphatic valves continuously required Piezo1 activity (Figure 3). All these in vivo loss-of-function studies defined the critical role of Peizo1 not only in lymphatic valve development but also in valve maintenance. These data once again support the positive feedback mechanism between fluid flow and the lymphatic valve–forming mechanotransduction mechanism: Lymphatic flow triggers lymphatic valve formation and maintenance, while lymphatic valves ensure proper lymphatic flow. Thus, a disruption of this delicate reciprocal feedback, for example because of surgical obstruction of lymphatic vessels in cancer patients (lymphadenectomy), would lead to lymphatic valve degeneration and eventually lymph stasis and lymphedema.

The interesting outcome of the gain-of-function studies in this paper elegantly mirrors the results of the loss-of-function studies. The ectopic upregulation of Piezo1 largely recapitulated the lymphatic valve gene profiles in cultured LECs without any fluid flow (Figure 5). Several molecular mechanisms could be envisioned. First, with an increased amount of Piezo1 protein, the cells could become much more sensitive to external force, such as subtle movement of culturing media or even their own movement during the culture period. Consistently, when reconstituted into lipid bilayers, purified Piezo1 proteins were able to mediate spontaneous and membrane tension–induced cationic currents (23, 42). Considering that Piezo1 forms a homotrimeric complex (43, 44), an alternative explanation could be that the increased number of Piezo1 monomers significantly facilitates the ion channel complex formation. A third mechanism could be that abundant Piezo1 protein may be able to overcome intrinsic negative regulations. For example, the Sarco/endoplasmic reticulum $Ca^{(2+)}$-ATPase (SERCA) family proteins, including SERCA2 isoform, have been identified as negative regulators of Piezo channels by acting through direct protein-protein interaction (45). Thus, more Piezo1 proteins could overcome such a SERCA-mediated suppression mechanism.

This gain of function could also be attained by chemical activation of Piezo1 in animals. Yoda1 is known to slow the inactivation phase of transient currents and sensitize Piezo1 response to external mechanical stimuli (37). Activation of Piezo1 using Yoda1 administration could accelerate lymphatic valve development in the mesenteries and skin of newborn mice (Figure 6). It is widely believed that lymphatic valves are formed at the anatomical sites where fluid flows are oscillatory or disturbed, such as vascular beds at branching points (20, 36). Importantly, although Yoda1 indeed promoted the valve formation process, when administered at the early stage, it did not seem to induce valve formation at the unusual, ectopic locations other than the expected sites. This suggests that Yoda1 or Piezo1 may be necessary, but not sufficient, for lymphatic valve development. Moreover, this is consistent with previous findings that Yoda1 only partially activates channels in the absence of external pressure (37) and our own data showing that Yoda1 treatment upregulated only some, but not all, lymphatic valve genes in cultured LECs without fluid flow (Figure 7).

Our studies in this report consistently found that regulation of ITGA9 expression was intriguingly unique compared with other lymphatic valve genes, providing some insights into possible Piezo1-independent force-sensing mechanisms. ITGA9 is known for its enriched expression in lymphatic valve leaflet ECs, although it is also moderately expressed in luminal LECs (3, 19, 20, 46–48). Protein and mRNA of ITGA9 were significantly upregulated in cultured LECs by OSS (Figure 4). Notably, Piezo1 was not essential for this OSS-induced upregulation of ITGA9, whereas it was for upregulation of all other genes tested.

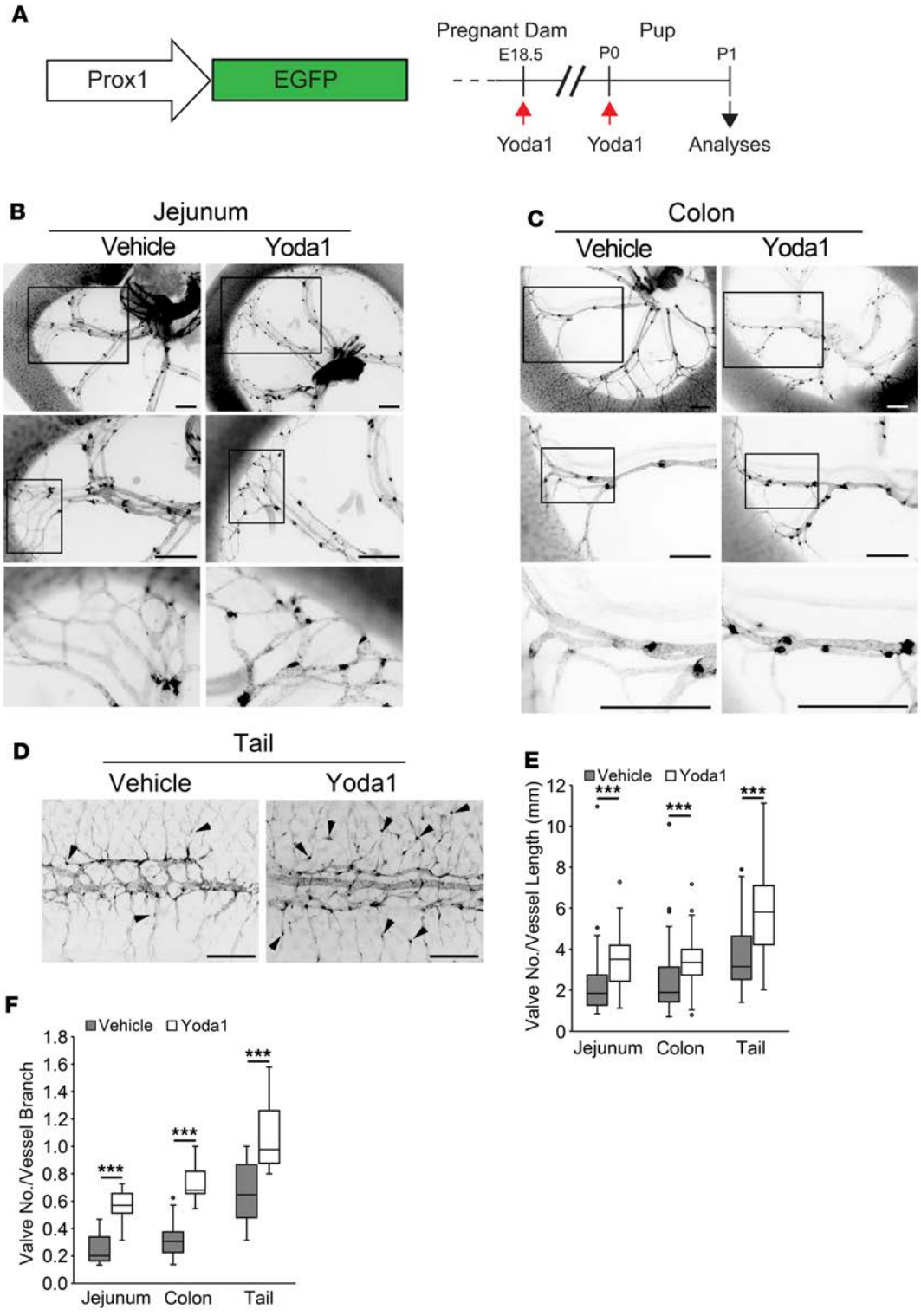

Figure 6. Activation of Piezo1 accelerates in vivo lymphatic valve formation. (**A**) Experimental design. Pregnant Prox1-EGFP females were i.p. injected with vehicle or Yoda1 (70 μg/kg) at E18.5 and then allowed to give birth to pups. Individual pups at P0 were injected once again with vehicle or Yoda1 (70 μg/kg) and then euthanized at P1 for lymphatic valve analyses. The effect of Yoda1 on developing mesenteric lymphatic valves was evaluated by selecting comparable anatomic locations in the (**B**) jejunum, (**C**) colon, and (**D**) tail skin of the vehicle or Yoda1-treated pups. (**E** and **F**) Images of the lymphatics were captured using EGFP signal, and lymphatic valve formation was quantified. The box plots depict the minimum and maximum values (whiskers), the upper and lower quartiles, and the median. The length of the box represents the interquartile range. More than 6 pups (mixed sex) were analyzed per group. Scale bars: 500 μm (**B**–**D**). ***$P < 0.001$, unpaired, 2-tailed t test compared with the vehicle-treated group (**E** and **F**).

This observation raised the notion that the OSS-induced upregulation of ITGA9 is not Piezo1 dependent, and this notion seems to be consistent with our finding that ectopic expression of Piezo1 did not increase ITGA9 expression (Figure 5). However, Yoda1 did upregulate ITGA9 in LECs in vitro as well as enhanced normal lymphatic valve formation in vivo (Figures 6 and 7). However, this Yoda1-induced ITGA9 upregulation in vitro did not require Piezo1 (Figure 7). Although these observations appear counterintuitive, a couple of possibilities could be considered. One is that the current experimental condition of OSS does not

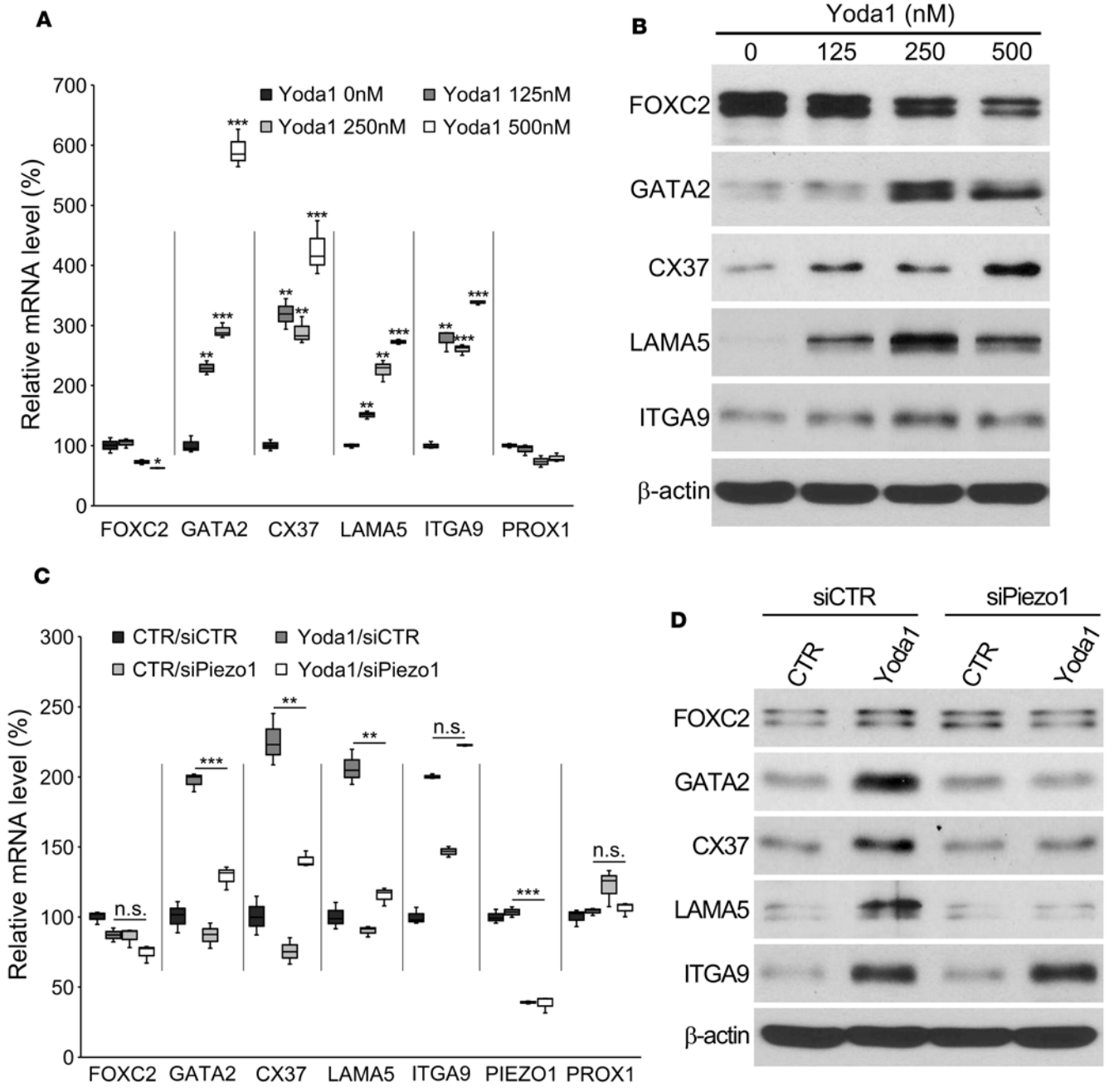

Figure 7. Yoda1 activates the expression of some lymphatic valve genes in a Piezo1-dependent manner. (**A** and **B**) Regulation of (**A**) mRNA and (**B**) protein of lymphatic valve genes in LECs by Yoda1 was determined by qPCR and Western blot analyses, respectively. Primary human LECs were treated by Yoda1 at the indicated concentrations for 24 hours. Yoda1 upregulated the expression of GATA2, CX37, LAMA5, and ITGA9 but not FOXC2 and PROX1. (**C** and **D**) Piezo1 is required for the Yoda1-induced upregulation of GATA2, CX37, and LAMA5 but not ITGA9. LECs were transfected with control siRNA (siCTR) or Piezo1 siRNA (siPiezo1) for 24 hours, followed by Yoda1 treatment (250 nM) for 24 hours, before isolation of (**C**) RNA or (**D**) whole-cell lysates for qPCR and Western blot analyses, respectively. The box plots depict the minimum and maximum values (whiskers), the upper and lower quartiles, and the median. The length of the box represents the interquartile range. $^{*}P < 0.05$; $^{**}P < 0.01$; $^{***}P < 0.001$; unpaired, 2-tailed *t* test.

precisely recapitulate the in vivo lymphatic valve–forming program and that this technical limitation may have caused some discrepancies among our in vitro and animal data. Another explanation is that ITGA9 may be upregulated in LECs by OSS through different mechanosensitive channels that could be stimulated, directly or indirectly, by Yoda1. Because Yoda1 does not activate Piezo2 (37, 49), Piezo2 can be excluded from the candidate list. Other stretch-activated channels, such as the transient receptor potential channel

subfamily C (TRPC) proteins (50–52), may be plausible candidates. Currently, neither the role of TRPC proteins in lymphatic development, nor the effect of Yoda1 on TRPC proteins, is known. Thus, it will be interesting and important to investigate these open questions.

During the review phase of this manuscript, a very similar study on the role of Piezo1 in lymphatic valve development was published by Nonomura et al. (53). The results from our and their studies are largely complementary and support the essential role of Piezo1 in lymphatic valve development. Yet, 2 points are worthy of discussion. First, these authors employed 2 constitutive endothelial Cre lines (*Tie2-Cre* and *Lyve1-Cre*), which delete Piezo1 in blood endothelial cells as well as LECs (53). The authors found gross phenotypes, including pleural effusion, similar to those displayed by human patients with *PIEZO1* loss-of-function mutations (28–30). In comparison, our study mainly used the *Prox1-CreER^{T2}* allele, which selectively targets LECs in a time-controlled manner by tamoxifen administration (Figures 1–3). Although our *Piezo1*-KO pups/mice showed growth retardation (Supplemental Figure 1), we did not detect pleural effusion or chylous ascites. These results may well be explained by the effects of different spatiotemporal deletion of *Piezo1* in our and their mouse models. The other point to note is that although our in vitro data revealed that Piezo1 regulated the key lymphatic valve signature genes, including FOXC2 and GATA2 (Figures 4 and 5), Nonomura et al. (53) found that Piezo1 was not required for the initiation of lymphatic valve formation. Although these discrepancies may be attributable to technical or experimental variations, further studies are required to resolve this difference. Nonetheless, both studies together clearly defined the essential role of the cell stretch sensor Piezo1 in lymphatic valve development.

Methods

Animal-related methods. Sources of the mice are: Prox1-EGFP (Tg[Prox1-EGFP]KY221Gsat, Mutant Mouse Resource and Research Centers, UCD, Davis, California, USA) (35), Prox1-tdTomato [Tg(Prox1-tdTomato)TA76Gsat/Mmucd, Mutant Mouse Resource and Research Centers] (31), *Prox1-CreER^{T2}* (a gift from Taija Mäkinen, Uppsala University, Uppsala, Sweden) (19), *Piezo1$^{fl/fl}$* (Piezo1$^{tm2.1Apat}$/J, The Jackson Laboratory) (32), Piezo1^{P1-tdT} (B6;129-Piezo1tm1.1Apat/J) (26), and Cdh5(PAC)-CreER^{T2} (a gift from Ralf Adams, University of Münster, Münster, Germany) (33). Mice were maintained in mixed outbred backgrounds. Both sexes were used for each experiment. Tamoxifen (MP Biomedicals) was dissolved in DMSO, mixed with sunflower seed oil (1 vol DMSO: 2 vol oil), and injected at 75 mg/kg once for pups and 3 times for young adults. For Figure 1, tamoxifen or vehicle was s.c. injected into neonatal mouse pups (P1), and tissue samples were harvested at P7 to analyze their genotypes and lymphatic valve development. Pups harboring *Prox1-tdTomato* and *Prox1-CreER^{T2}*, but lacking the *Piezo1$^{fl/fl}$* allele, were considered the CTR, while pups having *Prox1-tdTomato*, *Prox1-CreER^{T2}*, and *Piezo1$^{fl/fl}$* were marked as lymphatic *Piezo1*-KO (Piezo1$^{\Delta LEC}$). Yoda1 (MilliporeSigma) was dissolved in DMSO and then mixed with PBS (1.5 vol DMSO: 40 vol PBS) before injection at 70 μg/kg.

Cell culture–related reagents and assays. Human primary LECs were isolated from human foreskins and cultured in endothelial culturing media as previously described (54, 55). Primary cells less than 8 population doublings (passages) were used for the experiments in this study. The sources of the reagents are: Yoda1 (R&D Systems); tamoxifen (MP Biomedicals); and antibodies for FOXC2 (R&D Systems, AF5044), GATA2 (R&D Systems, AF2046), LAMA5 (Thermo Fisher Scientific, PA5-49930), CX37 (Abcam, ab181701), ITGA9 (R&D Systems, MAB4574), RFP/tdTomato (Rockland, 600-401-379), and β-actin (MilliporeSigma, A5441). Two sets of siRNA for human PIEZO1 (GCUGCCUCAAGUACUUCAUUU, GGCAGAAGAAGAAGAAGAUUU) were synthesized by GenePharma and independently used to confirm the effects of Piezo1 knockdown. Primer sequences used for the quantitative, qPCR are as follows: GATA2 (TTC AAT CAC CTC GAC TCG C/ GCT GTG CAA CAA GTG TGG/ FAM/AC TAT GCC A/ZEN/A CCC CGC TCA CG/3IABkFQ), FOXC2 (AGA TCA CCT TGA ACG GCA TC/ GCA CCT TGA CGA AGC ACT C/ 6-FAM/AA CAG CAT C/ZEN/C GCC ACA ACC TCT /3IABkFQ/), β-actin (TCA CCG AGC GCG GCT/ TAA TGT CAC GCA CGA TTT CCC/ JOE-CAG CTT CAC CAC CAC GGC CGA G-IBFQ1), CX37 (GTC ACT CCG GCC ATC GTC/ GGT GTG CTG ACG AAG AGG AA), LAMA5 (ATG GTT TCC CCA ACT GCC AA/ TAC AGG GAA CCT GTG CCT CA), ITGA9 (TCA ACA TGT GGC AGA AGG AGC CCA GAC AGG TGG CTT GTAT), PROX1 (TTT TAT ACC CGT TAT CCC AGCTC/ TGC GTA CTT CTC CAT CTG AAT/ 6-FAM/TG CTG AAG A/Zen/C CTACTT CTC CGA CGT AA/3IABkFQ), and PIEZO1 (GCA GCG CAT GAA CTT TCT GG/ CCA CTT GAT GAG TGC GGA GT).

Molecular and histological analyses. qPCR and Western blot analyses were performed using standard protocols as described (56). All fluorescence images were captured using a Leica stereomicroscope (Leica M165 FC) or a Zeiss ApoTome microscope (Zeiss AxioVision), except the images shown in Figure 2, C and D, which were obtained by a confocal microscope (Leica TCS SP5). Captured signals were inverted and expressed in grayscale using Adobe Photoshop CS5. Quantitative image analyses were performed using NIH ImageJ (NIH) software.

Flow generation. Oscillating flow was generated using a horizontal bidirectional shaker (MS-NOR-30, Major Science). A modified culture dish was made, as previously reported (7, 8), by adhering a 6-cm cell culture dish in the center of a 10-cm culture dish using a nontoxic medical silicone glue (A-100, medical silicone adhesive, Factor II, Inc.). Cells were seeded in the donut-shaped track and incubated for 24 hours under the static condition. Culture dishes were then horizontally rotated clockwise for 1 second and then counterclockwise for 1 second to generate reversing flow at maximum speed 100 rpm, 0.5 Hz, for approximately 6–24 hours. The approximate maximum wall shear stress was about 6 dyne/cm^2.

Statistics. An unpaired, 2-tailed *t* test was conducted using Microsoft Excel and GraphPad Prism 6 (GraphPad Software, Inc.) to determine whether the differences between the experimental and control groups were statistically significant. *P* value less than 0.05 was considered significant. Box-and-whisker plots were drawn using Microsoft Excel.

Study approval. All mouse methods were approved by the Institutional Animal Care and Use Committee, University of Southern California, Los Angeles, California. Isolation and culturing of human primary LECs from otherwise discarded, deidentified human foreskins were approved by the Institutional Review Board of the University of Southern California, Los Angeles, California.

Author contributions

DC, EP, EJ, BC, SL, JY, PMK, SL, YJH, CWC, and YW designed and performed the experiments and analyzed the data. CJK and NLJ provided the resources. AKW, LS, SRK, IBM, RSS, ITC, and YKH conceived, developed, and directed the project and/or wrote the paper.

Acknowledgments

This study was supported by NIH grants (R21EY026260, R01HL121036, R01HL141857, R21DE027891, and R01DK114645 to YH; R01HL131652 to RSS; and K08HL121191 to SRK) and by National Research Foundation of Korea (NRF-2018R1A2A1A05019550 to NLJ). We thank Taija Mäkinen (Uppsala University) and Ralf Adams (University of Münster) for sharing *Prox1-CreER^{T2}* and *Cdh5(PAC)-CreER^{T2}* mouse lines, respectively.

Address correspondence to: Young-Kwon Hong, Department of Surgery, University of Southern California, Norris Comprehensive Cancer Center, 1450 Biggy St. NRT6501, Los Angeles, California 90033, USA. Phone: 323.442.7825; Email: young.hong@usc.edu.

1. Breslin JW. Mechanical forces and lymphatic transport. *Microvasc Res*. 2014;96:46–54.
2. Bazigou E, Wilson JT, Moore JE. Primary and secondary lymphatic valve development: molecular, functional and mechanical insights. *Microvasc Res*. 2014;96:38–45.
3. Bazigou E, Makinen T. Flow control in our vessels: vascular valves make sure there is no way back. *Cell Mol Life Sci*. 2013;70(6):1055–1066.
4. Schmid-Schonbein GW. The second valve system in lymphatics. *Lymphat Res Biol*. 2003;1(1):25–29.
5. Chiu JJ, Chien S. Effects of disturbed flow on vascular endothelium: pathophysiological basis and clinical perspectives. *Physiol Rev*. 2011;91(1):327–387.
6. Schwartz MA, Simons M. Lymphatics thrive on stress: mechanical force in lymphatic development. *EMBO J*. 2012;31(4):781–782.
7. Choi D, et al. ORAI1 activates proliferation of lymphatic endothelial cells in response to laminar flow through Krüppel-like factors 2 and 4. *Circ Res*. 2017;120(9):1426–1439.
8. Choi D, et al. Laminar flow downregulates Notch activity to promote lymphatic sprouting. *J Clin Invest*. 2017;127(4):1225–1240.
9. Sessa WC. Molecular control of blood flow and angiogenesis: role of nitric oxide. *J Thromb Haemost*. 2009;7(suppl 1):35–37.
10. Boldock L, Wittkowske C, Perrault CM. Microfluidic traction force microscopy to study mechanotransduction in angiogenesis. *Microcirculation*. 2017;24(5):e12361.
11. Sabine A, Saygili Demir C, Petrova TV. Endothelial cell responses to biomechanical forces in lymphatic vessels. *Antioxid Redox Signal*. 2016;25(7):451–465.
12. Baeyens N, Bandyopadhyay C, Coon BG, Yun S, Schwartz MA. Endothelial fluid shear stress sensing in vascular health and disease. *J Clin Invest*. 2016;126(3):821–828.
13. Baeyens N, Schwartz MA. Biomechanics of vascular mechanosensation and remodeling. *Mol Biol Cell*. 2016;27(1):7–11.

14. Chatterjee S, Fujiwara K, Pérez NG, Ushio-Fukai M, Fisher AB. Mechanosignaling in the vasculature: emerging concepts in sensing, transduction and physiological responses. *Am J Physiol Heart Circ Physiol*. 2015;308(12):H1451–H1462.
15. Kazenwadel J, et al. GATA2 is required for lymphatic vessel valve development and maintenance. *J Clin Invest*. 2015;125(8):2979–2994.
16. Sabine A, et al. Mechanotransduction, PROX1, and FOXC2 cooperate to control connexin37 and calcineurin during lymphatic-valve formation. *Dev Cell*. 2012;22(2):430–445.
17. Sabine A, et al. FOXC2 and fluid shear stress stabilize postnatal lymphatic vasculature. *J Clin Invest*. 2015;125(10):3861–3877.
18. Cha B, et al. Mechanotransduction activates canonical Wnt/β-catenin signaling to promote lymphatic vascular patterning and the development of lymphatic and lymphovenous valves. *Genes Dev*. 2016;30(12):1454–1469.
19. Bazigou E, et al. Genes regulating lymphangiogenesis control venous valve formation and maintenance in mice. *J Clin Invest*. 2011;121(8):2984–2992.
20. Bazigou E, et al. Integrin-α9 is required for fibronectin matrix assembly during lymphatic valve morphogenesis. *Dev Cell*. 2009;17(2):175–186.
21. Udan RS, Dickinson ME. The ebb and flow of lymphatic valve formation. *Dev Cell*. 2012;22(2):242–243.
22. Janardhan HP, Milstone ZJ, Shin M, Lawson ND, Keaney Jr JF, Trivedi CM. Hdac3 regulates lymphovenous and lymphatic valve formation. *J Clin Invest*. 2017;127(11):4193–4206.
23. Coste B, et al. Piezo proteins are pore-forming subunits of mechanically activated channels. *Nature*. 2012;483(7388):176–181.
24. Kim SE, Coste B, Chadha A, Cook B, Patapoutian A. The role of Drosophila Piezo in mechanical nociception. *Nature*. 2012;483(7388):209–212.
25. Coste B, et al. Piezo1 and Piezo2 are essential components of distinct mechanically activated cation channels. *Science*. 2010;330(6000):55–60.
26. Ranade SS, et al. Piezo1, a mechanically activated ion channel, is required for vascular development in mice. *Proc Natl Acad Sci U S A*. 2014;111(28):10347–10352.
27. Li J, et al. Piezo1 integration of vascular architecture with physiological force. *Nature*. 2014;515(7526):279–282.
28. Lukacs V, et al. Impaired PIEZO1 function in patients with a novel autosomal recessive congenital lymphatic dysplasia. *Nat Commun*. 2015;6:8329.
29. Fotiou E, et al. Novel mutations in PIEZO1 cause an autosomal recessive generalized lymphatic dysplasia with non-immune hydrops fetalis. *Nat Commun*. 2015;6:8085.
30. Datkhaeva I, et al. Identification of novel PIEZO1 variants using prenatal exome sequencing and correlation to ultrasound and autopsy findings of recurrent hydrops fetalis. *Am J Med Genet A*. 2018;176(12):2829–2834.
31. Hong M, et al. Efficient assessment of developmental, surgical and pathological lymphangiogenesis using a lymphatic reporter mouse and its embryonic stem cells. *PLoS One*. 2016;11(6):e0157126.
32. Cahalan SM, Lukacs V, Ranade SS, Chien S, Bandell M, Patapoutian A. Piezo1 links mechanical forces to red blood cell volume. *Elife*. 2015;4:e07370.
33. Wang Y, et al. Ephrin-B2 controls VEGF-induced angiogenesis and lymphangiogenesis. *Nature*. 2010;465(7297):483–486.
34. Giannotta M, Trani M, Dejana E. VE-cadherin and endothelial adherens junctions: active guardians of vascular integrity. *Dev Cell*. 2013;26(5):441–454.
35. Choi I, et al. Visualization of lymphatic vessels by Prox1-promoter directed GFP reporter in a bacterial artificial chromosome-based transgenic mouse. *Blood*. 2011;117(1):362–365.
36. Norrmén C, et al. FOXC2 controls formation and maturation of lymphatic collecting vessels through cooperation with NFATc1. *J Cell Biol*. 2009;185(3):439–457.
37. Syeda R, et al. Chemical activation of the mechanotransduction channel Piezo1. *Elife*. 2015;4:e07369.
38. Zhao S, et al. Synergistic effects of fluid shear stress and cyclic circumferential stretch on vascular endothelial cell morphology and cytoskeleton. *Arterioscler Thromb Vasc Biol*. 1995;15(10):1781–1786.
39. Kim DH, Heo SJ, Kang YG, Shin JW, Park SH, Shin JW. Shear stress and circumferential stretch by pulsatile flow direct vascular endothelial lineage commitment of mesenchymal stem cells in engineered blood vessels. *J Mater Sci Mater Med*. 2016;27(3):60.
40. Moore JE, et al. A device for subjecting vascular endothelial cells to both fluid shear stress and circumferential cyclic stretch. *Ann Biomed Eng*. 1994;22(4):416–422.
41. Owatverot TB, Oswald SJ, Chen Y, Wille JJ, Yin FC. Effect of combined cyclic stretch and fluid shear stress on endothelial cell morphological responses. *J Biomech Eng*. 2005;127(3):374–382.
42. Syeda R, et al. Piezo1 channels are inherently mechanosensitive. *Cell Rep*. 2016;17(7):1739–1746.
43. Ge J, et al. Architecture of the mammalian mechanosensitive Piezo1 channel. *Nature*. 2015;527(7576):64–69.
44. Zhao Q, et al. Structure and mechanogating mechanism of the Piezo1 channel. *Nature*. 2018;554(7693):487–492.
45. Zhang T, Chi S, Jiang F, Zhao Q, Xiao B. A protein interaction mechanism for suppressing the mechanosensitive Piezo channels. *Nat Commun*. 2017;8(1):1797.
46. Altiok E, et al. Integrin α-9 mediates lymphatic valve formation in corneal lymphangiogenesis. *Invest Ophthalmol Vis Sci*. 2015;56(11):6313–6319.
47. Høye AM, Couchman JR, Wewer UM, Fukami K, Yoneda A. The newcomer in the integrin family: integrin ,α9 in biology and cancer. *Adv Biol Regul*. 2012;52(2):326–339.
48. Mishima K, et al. Prox1 induces lymphatic endothelial differentiation via integrin α9 and other signaling cascades. *Mol Biol Cell*. 2007;18(4):1421–1429.
49. Lacroix JJ, Botello-Smith WM, Luo Y. Probing the gating mechanism of the mechanosensitive channel Piezo1 with the small molecule Yoda1. *Nat Commun*. 2018;9(1):2029.
50. Inoue R, Jian Z, Kawarabayashi Y. Mechanosensitive TRP channels in cardiovascular pathophysiology. *Pharmacol Ther*. 2009;123(3):371–385.
51. Barritt G, Rychkov G. TRPs as mechanosensitive channels. *Nat Cell Biol*. 2005;7(2):105–107.
52. Dalrymple A, Mahn K, Poston L, Songu-Mize E, Tribe RM. Mechanical stretch regulates TRPC expression and calcium entry

in human myometrial smooth muscle cells. *Mol Hum Reprod*. 2007;13(3):171–179.
53. Nonomura K, et al. Mechanically activated ion channel PIEZO1 is required for lymphatic valve formation. *Proc Natl Acad Sci U S A*. 2018;115(50):12817–12822.
54. Shin JW, et al. Prox1 promotes lineage-specific expression of fibroblast growth factor (FGF) receptor-3 in lymphatic endothelium: a role for FGF signaling in lymphangiogenesis. *Mol Biol Cell*. 2006;17(2):576–584.
55. Lee S, et al. Prox1 physically and functionally interacts with COUP-TFII to specify lymphatic endothelial cell fate. *Blood*. 2009;113(8):1856–1859.
56. Yoo J, et al. Kaposin-B enhances the PROX1 mRNA stability during lymphatic reprogramming of vascular endothelial cells by Kaposi's sarcoma herpes virus. *PLoS Pathog*. 2010;6(8):e1001046.